Chapter V

[Bis(picolinate-κ^2*N:O*)Copper(II)] di(benzene-1,3,5- tricarboxylic acid): hydrothermal synthesis, structural characterization, magnetic properties and DFT study*

5.1. Introduction

The diversity in the structure of Cu(II) complexes is highly related to its d^9 system. This allows it to have variety of coordination polyhedra with significantly different geometries. Cu(II) is found in mononuclear, dinuclear and polynuclear species with diverse structures.[1] The d^9 system plays crucial role in various characterization methods (electronic spectroscopy, electron paramagnetic resonance and magnetic susceptibility) that are connected to the Cu(II) chemistry.[2,42] In the past decades, a growing interest in the field of magneto-chemistry has been observed, attributed due to huge practical applications of various magnetic materials. The interactions of the unpaired electrons in d^9 system may lead to the formation of magnetic materials like paramagnetic, antiferromagnetic, ferromagnetic species, *etc.*[3, 42]

Recently, chemists around the world have shown tremendous interest in synthesizing metal-organic hybrid complexes. This extensive interest to design, synthesize and explore potential applications of such hybrid complexes stemmed from intriguing structural features, fascinating compositional variability and charming theoretical and practical applications in various fields like adsorption, chemical separation catalysis, magnetism, *etc.*[4-6] The carboxylates of transition metals shows variety in coordination modes due to the ability of carboxylic group to form polymer or cluster[7] involving carboxyl group. The picolinate ion has an inherent property of forming chelate rings leading to the formation of stable mononuclear or polynuclear complexes. The pyridine N-atom and the carboxylate O-atoms of the picolinic acid moiety are fairly capable of forming complexes with a variety of transition metal ions. Metal complexes involving of bio-active ligands are now-a-days, targeted for developing new drugs. Metal complexes of picolinic acid have been the area of intense research stemmed from superb coordination flexibilty and wide range of

 *Published in J. Mol. Struc 1165 (2018) 228-235 and CCDC No. 1487798

physiological properties, like insulinomimetic activity[8-14] and also in designing new metallo-pharmaceuticals.[15-19] The coordination number, oxidation state and structure of such complexes influence their biological and physico-chemical properties.[17] Benzene-1,3,5-tricarboxylic acid (trivially known as trimesic acid, TMA) being rigid and planar, has been extensively used in its anionic form. This anionic form acts as a bridging ligand for the synthesis of metal-organic hybrid materials ranging from 1D to 3D. Thus TMA plays vital role in defining the and functional versatility of the hybrid complexes.[20-22]

Hydrothermal method is regarded as one of the best methods employed to synthesize dislocation free pure single crystals of organic-inorganic hybrid complexes. This method is cheap and uses environment friendly water as reaction medium. Thus synthesis of metal-organic hybrid complexes using hydrothermal technique is in agreement with green chemistry requirements.[23] Herein this chapter the hydrothermal synthesis of hybrid complex [Bis(picolinate-$\kappa^2N:O$)Copper(II)] di(benzene-1,3,5-tricarboxylic acid; using $Cu(NO_3)_2.3H_2O$, picolinic acid and benzene-1,3,5-tricarboxylic acid (trimesic acid, TMA) has been reported. The synthesized complex was characterized by analytical, physico-chemical and spectroscopic techniques like FTIR spectroscopy, single crystal X-ray diffraction, FESEM, EPR, SQUID, TGA and DFT study.

5.2. Experimental Section

5.2.1. Materials and Methods

Hydrothermal synthesis of the title complex was performed in a 10 mL stainless steel Teflon-lined autoclave at 150 °C and under autogenous pressure. Copper nitrate [$Cu(NO_3)_2 \cdot 3H_2O$], picolinic acid, trimesic acid and triply distilled de-ionized water (specific conductance < $1 \cdot 10^{-6}$ $S \cdot cm^{-1}$ at 25 °C) were used in this synthesis. The source and purity of the chemicals used in the synthesis of title complex has been detailed in chapter II. The elemental micro-analyses (C, H and N) were performed using Perkin–Elmer (Model 240C) analyzer. AAS (Varian, SpectrAA 50B) was used for the determination of Cu-content using standard Cu-solution procured from Sigma-Aldrich, Germany. Single crystal X-ray diffraction study was performed using Oxford diffractometer equipped with CCD camera. The IR spectrum in KBr pellet was recoded using Perkin-Elmer Spectrum FT-IR spectrometer (RX-1)

operating in the region 4000 to 400 cm^{-1} at ambient temperature. Ever Cool 7 Tesla SQUID magnetometer was used for the study of magnetic susceptibility of the powdered crystalline sample. The X-band EPR of the synthesized complex was recorded using EPR magnetometer (JEOL, JES-X3 FA200) operating in the field range of 266.66 mT to 386.66 mT. Thermal stability and behaviour of the title complex was studied by thermogravimetric analysis (TGA) and differential thermogravimetry (DTG) analysis. The data were recorded using TGA instrument (Q500 V20.10 Build 36) in N_2 atmosphere with 6.619 mg of the complex. The crystal morphology was studied using Field Emmission Scaning Electron Microscopy (FESEM, INSPECT F50, FEI, The Netherland). The detailed descriptions of the various analytical and spectroscopic methods and instruments have been discussed in chapter II.

5.2.2. Synthesis of [Bis(picolinate-κ^2N:O)Copper(II)] di(benzene-1,3,5-tricarboxylic acid

A mixture of $Cu(NO_3)_2.3H_2O$ (0.2416 g, 1mmol), picolinic acid (0.123 g, 1mmol) and benzene-1,3,5-tricarboxylic acid (trimesic acid) (0.21 g, 1mmol) was first pulverized using agate pastle and mortar. The pulverized mixture was then transferred to a 10 mL Teflon-lined stainless steel autoclave and 4 mL of water (triply distilled de-ionized) was added and the mixture thus obtained was stirred for 30 min to a suspension. The autoclave was sealed and placed in an automated hot air oven; maintained at 150 ^oC and heated for 48 h. After 48 hours, the autoclave was subjected to natural cooling (for about 6 h) at room temperature. The pH = 3 of the suspension before and after the reaction remained the same. Then the mixture was filtered and the residue thus obtained was repeatedly washed with sufficient amount of de-ionized water. The residue with the blue crystals was washed with adequate amount of ethanol to remove any un-reacted picolinic acid and TMA and the crystals thus obtained were dried in air. The single crystals were separated and collected by hand picking under a microscope (40x). The complex was found insoluble in common conventional solvents and it did not melt up to 300 ^oC. Yield: 85% (based on Cu). Elemental analysis calcd (%) for $[Cu(C_{30}H_{20}N_2O_{16})]$: C 49.49, H 2.77, N 3.85, Cu 8.73; found: C 48.75, H 2.69, N 3.68, Cu 8.35.

5.2.3. X-ray crystallographic measurements

Crystal data collection and structure refinement are summarized in Table 5.1. The details of data collection using single crystal X-ray diffractometer and structural refinement using related softwares and programmes are discussed in chapter II. The selected bond lengths and angles of the complex are summarized in Table 5.2. The hydrogen bond geometry and their corresponding symmetry codes are listed in Table 5.3. The fractional atomic coordinates and isotropic or equivalent isotropic displacement parameters, atomic displacement parameters and geometric parameters are listed in tables 5.4 to 5.6, respectively. The parameters summarized in these tables give clear insight into the geometry and coordination of the synthesized complex.

Table 5.1. Crystallographic parameters of the complex

Crystal Data	
Chemical formula	$[Cu(C_{30}H_{20}N_2O_{16})]$
M_r	728.03
Crystal system, Space group	Monoclinic, P 1 21/c 1
Temperature (K)	293
a , b, c (Å)	4.9853 (4), 13.1082 (5), 21.6616 (8)
β (°)	90, 91.23 (6), 90
V (Å^3)	1415.22(14)
Z	4
Radiation type	Mo $K\alpha$
μ (mm^{-1})	1.784
Crystal size (mm)	$0.033\times0.052\times0.726$
Data collection	
Diffractometer	Oxford Diffraction Gemini
Absorption correction	Analytical
T_{min}, T_{max}	0.948, 0.972
No. of measured, independent and observed [$I > 2\sigma(I)$] reflections	2423, 3429, 2662
R_{int}	0.014
θ_{max},θ_{min}	29.245, 3.108
h	-6 →6
k	-17 →17

l	-29 →28
Refinement	
$R(F^2)> 2\sigma(F^2)$, $wR(F^2)$, S	0.0415, 0.0462, 1.0610
No. of reflections	2662
No. of parameters	224
No. of restraints	0
$\Delta\rho_{max}$, $\Delta\rho_{min}$ (e Å^{-3})	0.61, -0.45

Table 5.2. Selected bond lengths and angles (Å, ^{o})

Cu1-N6	1.959 (2)	O13-C12	1.204 (3)
Cu1-O2	1.928 (2)	N6-Cu1-O2	83.68 (8)
O2-C3	1.271 (3)	N6-Cu1-O2	96.32 (8)
C3-O4	1.235 (3)	O2-Cu1-O2	179.99 (4)
O11-C12	1.307 (3)	N6-Cu1-N6	179.99 (4)

Table 5.3. Hydrogen-bond geometry (Å, ^{o})

$D-\mathrm{H}\cdots A$	$D-\mathrm{H}$	$\mathrm{H}\cdots A$	$D\cdots A$	$D-\mathrm{H}\cdots A$
C7-H71…O13	0.937	2.462	3.386(3)	168.80
C10-H101…O19i	0.947	2.574	3.478(3)	159.76
C20-H201…O4ii	0.932	2.529	3.263(3)	135.90
O11-H111…C3iii	0.831	2.581	3.401(3)	169.45
O11-H111…04iii	0.831	1.800	2.610(3)	164.42
O25-H251…O4ii	0.827	2.552	3.181(3)	133.83
O25-H251…C20	0.827	2.175	2.722(3)	123.70
O18-H181…O19iv	0.830	2.568	3.323(3)	151.90

Symmetry codes: i) $x-2,-y-1/2,z-1/2$ ii) $x+2,-y-1/2,z+1/2$, iii) $-x,-y,-z+1$, iv) $x-1,y,z$

Table 5.4. Fractional atomic coordinates and isotropic or equivalent isotropic displacement parameters (Å^2)

	x	*y*	*z*	U_{iso}*/U_{eq}
Cu1	0.0000	0.0000	0.5000	0.0409
O2	-0.2686 (4)	-0.04638 (13)	0.44099 (10)	0.0518
C3	-0.2616 (5)	-0.14124 (18)	0.42905 (11)	0.0361
O4	-0.4142 (4)	-0.18441 (13)	0.39174 (9)	0.0456
C5	-0.0502(5)	-0.20146 (17)	0.46364 (10)	0.0317
N6	0.1090 (4)	-0.14359 (14)	0.50062 (9)	0.0330
C7	0.3042 (5)	-0.18713 (19)	0.53449 (11)	0.0367
C8	0.3442 (5)	-0.2915 (2)	0.53338 (12)	0.0404
C9	0.1790 (6)	-0.35133 (19)	0.49651(12)	0.0409
C10	-0.0205 (5)	-0.30592 (18)	0.46021(12)	0.0390
O11	0.7334 (4)	0.07703(16)	0.67985 (10)	0.0562
C12	0.8290 (5)	-0.0120 (2)	0.66455 (12)	0.0392
O13	0.7758 (5)	-0.05778 (18)	0.61767 (10)	0.0638
C14	1.0221 (5)	-0.05449 (18)	0.71239 (11)	0.0343
C15	1.0671 (5)	-0.00769 (17)	0.76941 (11)	0.0329
C16	1.2571 (5)	-0.04964 (17)	0.80937 (10)	0.0321
C17	1.3082 (4)	-0.00083 (17)	0.86956 (9)	0.0288
C18	1.1438 (5)	0.05891 (18)	0.88834 (10)	0.0589
O19	1.5149 (5)	-0.02276 (15)	0.89789 (9)	0.0536
C20	1.4047 (5)	-0.13548 (17)	0.79554 (11)	0.0345
C21	1.3486 (5)	-0.18053 (17)	0.73923 (11)	0.0353
C22	1.1603 (5)	-0.14278 (18)	0.69748 (11)	0.370
C23	1.5009 (5)	-0.27209 (17)	0.72246 (11)	0.0337
O24	1.4055 (5)	-0.32712 (17)	0.68210 (11)	0.0655
O25	1.7135 (5)	-0.28770 (17)	0.74950 (11)	0.0623
H71	0.4157	-0.1444	0.5584	0.0432*
H81	0.4823	-0.3206	0.5567	0.0470*

H91	0.2061	-0.4222	0.4956	0.0481*
H101	-0.1329	-0.3450	0.4335	0.0461*
H151	0.9725	0.0507	0.7803	0.0377*
H201	1.5362	-0.1610	0.8226	0.0401*
H221	1.1289	-0.1754	0.6600	0.0431*
H111	0.6190	0.1008	0.6554	0.0828*
H251	1.6938	-0.2575	0.7826	0.0934*
H181	1.0059	0.0258	0.8797	0.0893*

Table 5.5. Atomic displacement parameters ($Å^2$)

	U11	*U22*	*U33*	*U23*	*U13*	*U12*
Cu1	0.0447(3)	0.0248(2)	0.0521(3)	-0.00639(18)	-0.02390(19)	0.00324(18)
O2	0.0564(12)	0.0296(9)	0.0679(13)	-0.0083(8)	-0.0359(10)	0.0053(8)
C3	0.0399(13)	0.0325(11)	0.0355(12)	-0.0024(9)	-0.0094(10)	0.0010(10)
O4	0.0515(11)	0.0366(9)	0.0476(10)	-0.0079(7)	-0.0228(9)	0.0013(8)
C5	0.0348(12)	0.0298(10)	0.0302(10)	-0.0030(8)	-0.0047(9)	0.0001(9)
N6	0.0359(10)	0.0284(9)	0.0342(10)	-0.0019(7)	-0.0089(8)	0.0017(8)
C7	0.0390(13)	0.0363(12)	0.0343(12)	-0.0015(9)	-0.0088(10)	0.0032(10)
C8	0.0452(14)	0.0408(13)	0.0349(12)	0.0063(10)	0.0058(11)	0.0100(11)
C9	0.0511(15)	0.0297(11)	0.0421(13)	0.0028(10)	0.0020(11)	0.0071(10)
C10	0.0453(14)	0.0305(11)	0.0408(13)	-0.0033(9)	-0.0062(11)	-0.0010(10)
O11	0.0654(13)	0.0503(11)	0.0516(11)	-0.0096(9)	-0.0280(10)	0.0198(10)
C12	0.0332(12)	0.0451(14)	0.0389(12)	-0.0038(10)	-0.0083(10)	0.0011(10)
O13	0.0635(14)	0.0702(14)	0.0564(13)	-0.0230(11)	-0.0298(11)	0.0188(11)
C14	0.0324(12)	0.0352(12)	0.0349(12)	0.0003(9)	-0.0046(9)	-0.0030(9)
C15	0.0332(11)	0.0293(10)	0.0361(11)	-0.0023(9)	-0.0015(9)	-0.0001(9)
C16	0.0362(12)	0.0293(11)	0.0307(11)	0.0004(8)	-0.0023(9)	-0.0061(9)
C17	0.0367(11)	0.0260(9)	0.0237(9)	0.0002(8)	-0.0012(8)	-0.0039(10)

O18	0.0579(13)	0.0711(14)	0.0474(11)	-0.0198(10)	-0.0043(10)	0.0046(11)
O19	0.0667(13)	0.0475(11)	0.0455(11)	-0.0008(8)	-0.0233(10)	0.0004(9)
C20	0.0359(12)	0.0307(11)	0.0366(12)	0.0036(9)	-0.0022(10)	0.0015(9)
C21	0.0396(13)	0.0288(11)	0.0377(12)	0.0006(9)	0.0046(10)	0.0005(9)
C22	0.0393(13)	0.0364(12)	0.0351(12)	-0.0054(9)	-0.0019(10)	-0.0026(10)
C23	0.0394(13)	0.0257(10)	0.0362(12)	-0.0005(9)	0.0064(10)	0.0057(9)
O24	0.0868(17)	0.0481(12)	0.0615(13)	-0.0159(10)	0.0002(12)	0.0139(12)
O25	0.0588(14)	0.0491(12)	0.0790(16)	-0.0055(11)	0.0019(12)	0.0186(10)

Table 5.6. Geometric parameters (Å, °)

Cu1-O2	1.928(2)	C12-C14	1.506(3)
Cu1-N6	1.959(2)	C14-C15	1.393(3)
O2-C3	1.271(3)	C14-C22	1.388(3)
C3-O4	1.235(3)	C15-C16	1.384(3)
C3-C5	1.504(3)	C16-C17	1.469(3)
C5-N6	1.349(3)	C16-C20	1.381(3)
C5-C10	1.379(3)	C17-O18	1.210(3)
N6-C7	1.334(3)	C17-O19	1.222(3)
C7-C8	1.383(4)	C20-C21	1.379(3)
C9-C10	1.388(4)	C21-C22	1.381(4)
O11-C12	1.307(3)	C23-O24	1.222(3)
C12-O13	1.204(3)	C23-O25	1.217(3)
N6-Cu1-O2	83.68(8)	O11-C12-O13	125.7(2)
N6-Cu1-O2	96.3(8)	O11-C12-C14	112.8(2)
O2-Cu1-O2	179.994(	O13-C12-C14	121.5(2)
N6-Cu1-N6	179.994	C12-C14-C15	122.4(2)
O2-Cu1-N6	96.32(9)	C12-C14-C22	117.5(2)
O2-Cu1-N6	83.68(9)	C15-C14-C22	120.1(2)
Cu1-O2-C3	115.00(16)	C14-C15-C16	118.3(2)

O2-C3-O4	124.3(2)	C15-C16-C17	119.0(2)
O2-C3-C5	115.7(2)	C15-C16-C20	123.3(2)
O4-C3-C5	120.1(2)	C17-C16-C20	117.7(2)
C3-C5-N6	113.4(2)	C16-C17-O18	118.3(2)
C3-C5-C10	124.7(2)	C16-C17-O19	118.1(2)
N6-C5-C10	121.9(2)	O18-C17-O19	123.6(2)
C5-N6-Cu1	112.13(16)	C16-C20-C21	116.2(2)
C5-N6-C7	119.9(2)	C20-C21-C23	118.2(2)
Cu1-N6-C7	127.85(16)	C22-C21-C23	118.6(2)
N6-C7-C8	121.1(2)	C14-C22-C21	118.7(2)
C7-C8-C9	119.2(2)	C21-C23-O24	117.6(2)
C8-C9-C10	119.7(2)	C21-C23-O25	117.9(2)
C9-C10-C5	118.1(2)	O24-C23-O25	124.5(2)

5.2.4. Theoretical Methods

Density functional theory (DFT) has proved to be an effective tool for electronic properties of molecules, structural determination, ionization energies atomization energies, vibrational frequencies, *etc*.[24-26] The synthesized complex was optimized DFT with B3LYP hybrid functional[27-28] using Gaussian 09 programme package[29] and LANL2DZ basis set was used for Cu(II) ion. Single crystal X-ray diffraction provided the initial structure for the fragments of title complex. The molecular geometries were optimized without any symmetry constraints. Harmonic vibrational frequencies were calculated at B3LYP level of theory to confirm the local minima character of the structures. To understand the stability, electronic properties and molecular orbital (MO) analysis was performed at the same level of theory.

5.3. Results and discussion

5.3.1. Crystal structure of [Bis(picolinate-κ^2N:O)Copper(II)] di(benzene-1,3,5-tricarboxylic acid

Fig 5.1 reveals that the asymmetric unit of the complex consists of two 2-picolinic acid coordinating the Cu(II) ion. It is evident from Fig 5.1 that Cu(II)

occupies the centre of symmetry forms a five member chelate ring when coordinated to picolinic moieties through pyridinium N-atom and carboxylate O-atoms simultaneously. The geometry of the complex is slightly distorted square planar (Fig 5.2 and 5.3). The complex crystallise in monoclinic crystal system with space group is P1 21/c 1.

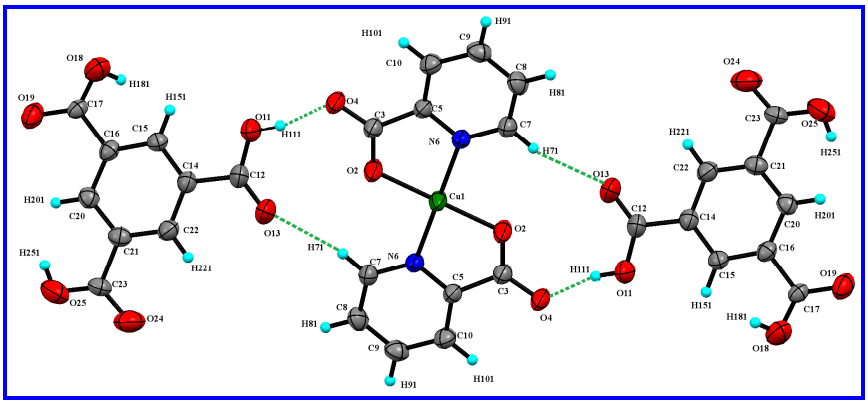

Fig 5.1. Asymmetric unit of the complex showing the atom numbering scheme.Displacement ellipsoids are drawn at 50% probability level.

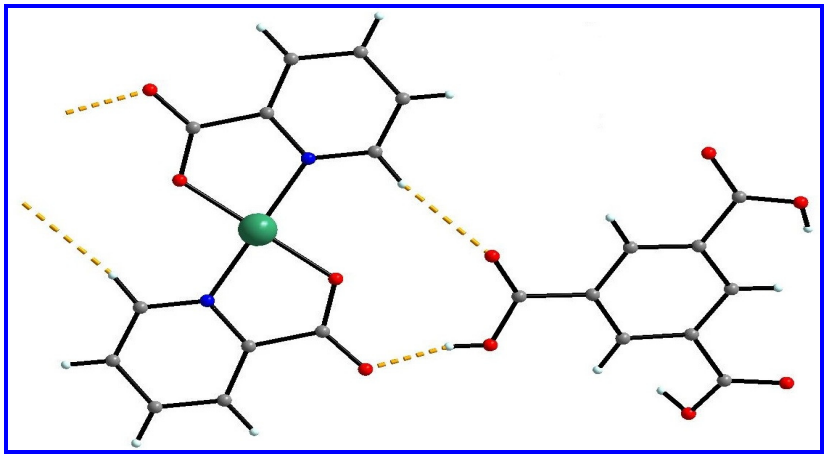

Fig 5.2. Coordination geometry of Cu(II) ion in the complex. Color scheme: green, Cu; red, O; blue, N; grey, C and sky blue, H.

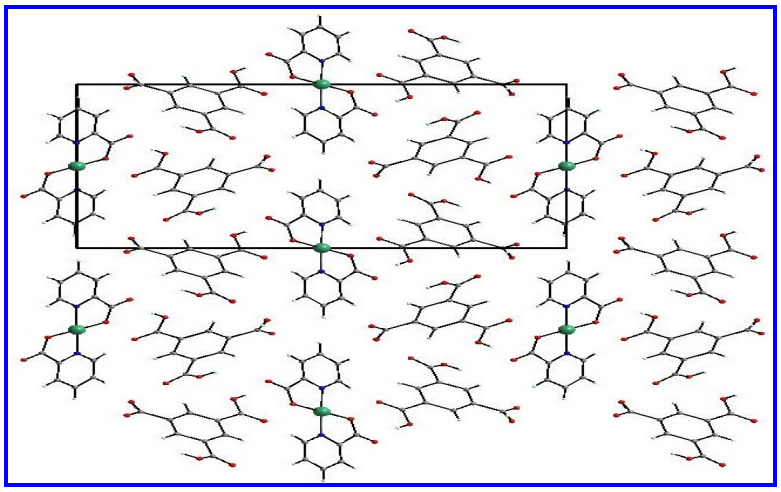

Fig 5.3. A view approximately normal to the chain along the *c*-axis showing.
Colors: grey, C; blue, N; green, Cu; red, O; and sky blue, H.

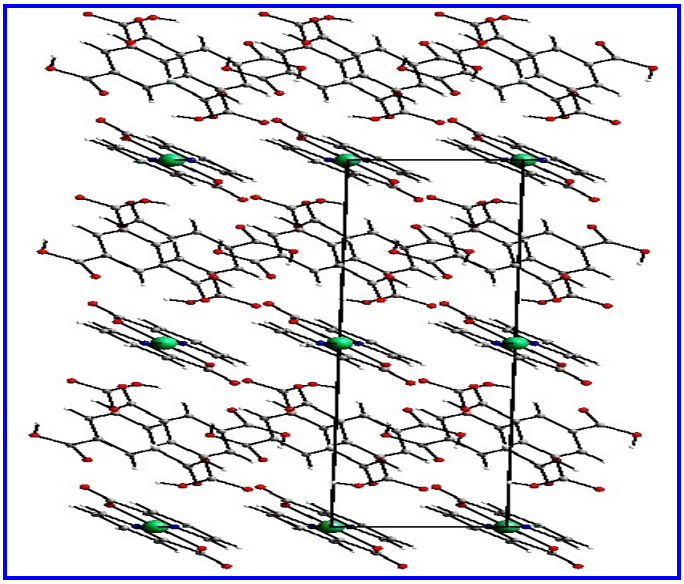

Fig 5.4. A view approximately along the *b*-axis.
Color: grey, C; blue, N; green, Cu; red, O; and sky blue, H.

The Cu(II) ion situated on crystallographic inversion centre is coordinated to two picolinate ligands placed in the equatorial plane. The extensive hydrogen bond shown in Figs 5.1 and 5.4 involving trimesic acid is responsible for the exceptional stability of the complex. Interestingly, this reaction failed to give the crystal in absence of trimesic acid under the same applied reaction condition. The Cu1–N6 bond distance of 1.959 Å and the bond angles formed around Cu(II) ion,

involving trans pairs of donor atoms found to be slightly distorted. The presence of TMA moieties is probably responsible for the distortion in geometry of the complex. The N or O atoms of coordination from the two 2-picolinic acid molecules are equivalent.

5.3.2. FTIR spectroscopy

The FTIR spectrum of the synthesized complex was shown in Fig 5.7. The asymmetric ν_{as} (COO-) and symmetric ν_s (COO-) stretching vibrations of carboxylate group appeared at 1718 cm^{-1} and 1320 cm^{-1} respectively. The difference ($\Delta\nu = \nu_{as} - \nu_{sym}$)= 398 cm^{-1} indicates monodentate carboxylate coordination.[30-31] The high value of $\Delta\nu$ (> 200 cm-1) suggests highly asymmetric bridging ("pseudo-monodentate" coordination).[30] This coordination mode is consistent with the crystal structure of the complex.

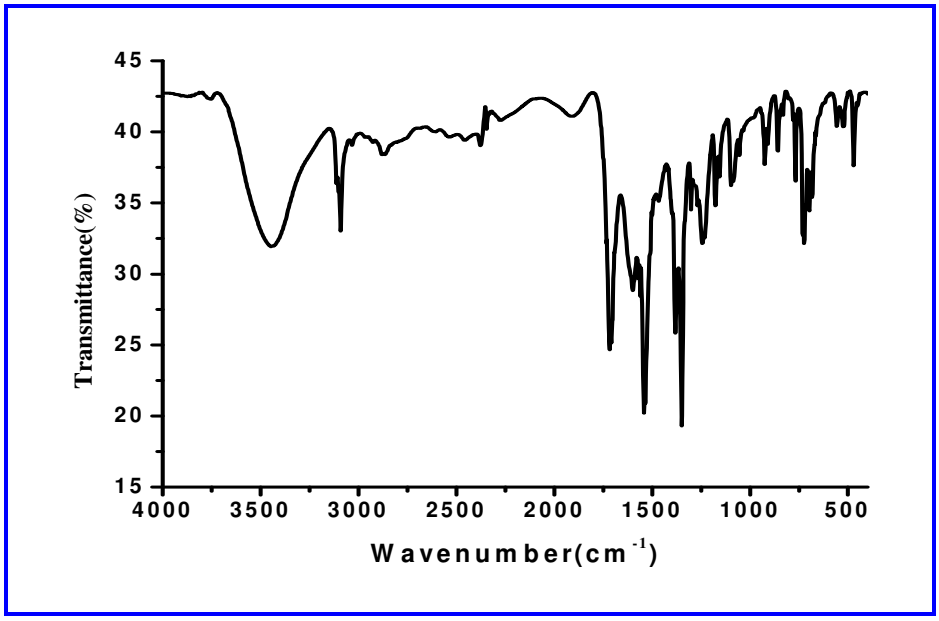

Fig 5.5. FTIR spectrum of the complex.

The sharp peak at 1599 cm^{-1} indicates N, O-chelation,[32] involving the pyridinium N-atom of picolinate ligand. The peak appearing at 423 cm^{-1} is assigned to Cu-N bond.[33-34] The broad band appearing at 471 cm^{-1} indicates presence of Cu-O bond.[33-34] The sharp peak at 3091cm^{-1} is due to the aromatic C-H stretching vibrations of picolinic acid moiety.[32]

5.3.3. Magnetic properties

The X-band EPR spectrum of the complex was recorded in the field range of 266.66 –386.66 mT. Fig 5.8 shows the X-band EPR spectrum of the complex. For the complex calculations show that $g_{\parallel} = 2.29$ and $g_{\perp} = 2.099$ and the fact that $g_{\parallel} > g_{\perp} > 2.003$ suggests that the unpaired electron of d^9 of Cu(II) belongs to $d_{x^2-y^2}$ supporting the square planar geometry of Cu(II) in the complex.[35] Further, magnetic susceptibilities of powdered crystalline sample were measured by SQUID magnetometer in the temperature range $T = 2$ to 300 K in an applied magnetic field of 100 Oe.

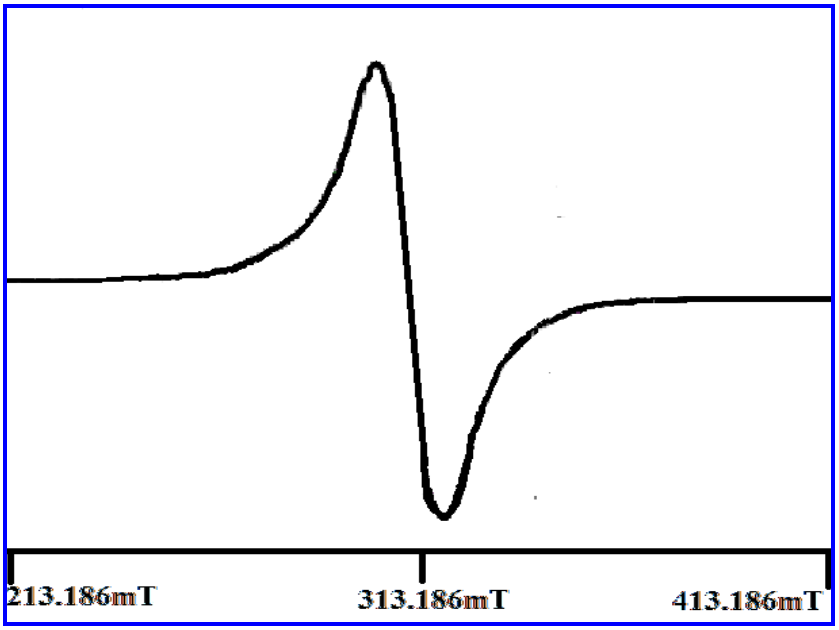

Fig. 5.8. EPR spectrum of the complex.

The magnetic susceptibility of the title complex was measured on the polycrystalline sample from 2 to 300 K under an applied magnetic field of 100 *Oe*. As shown in Fig. 5.9, the $\chi_m T$ value gradually increases with lowering of temperature.

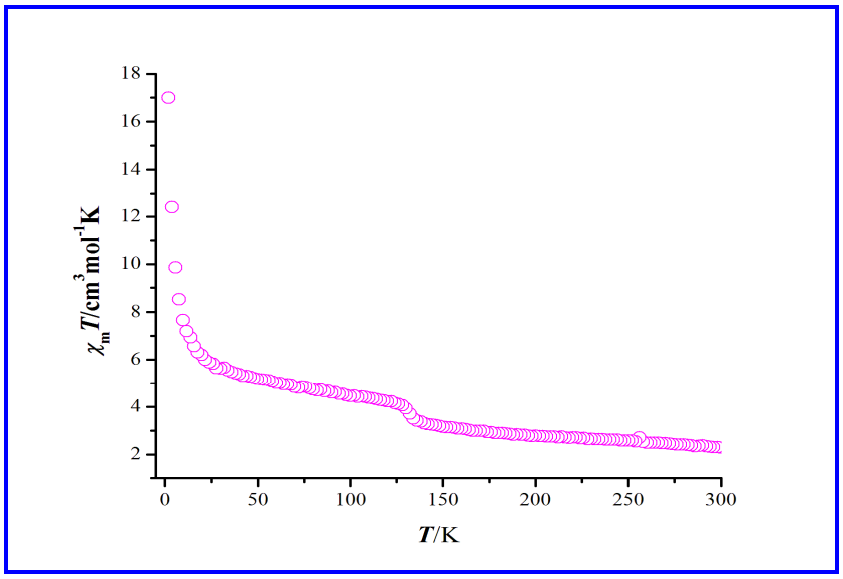

Fig 5.7. Temperature dependence of χ_{mol} for the complex.

The value of $\chi_m T$ steadily increases until above 20 K and then sharply reaches a maxima of 17 cm^3 mol^{-1} K at 2 K. The temperature dependent $\chi_m T$ behavior reveals the overall ferromagnetic behavior for the complex.

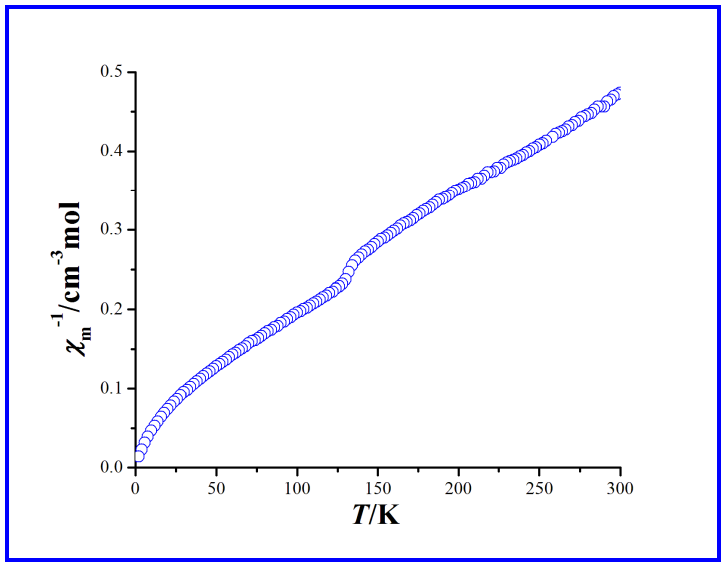

Fig 5.8. Temperature dependence of χ_m^{-1} for the complex.

Fig. 5.10 shows almost a linear variation of $1/\chi_m$ with temperature and in accordance with Curie–Weiss law. The Weiss constant (θ = –35 K) was determined from a linear fit of the data (Fig 5.10). The negative value of θ indicates weak anti-ferromagnetic

interactions in the complex at low temperatures. However, $\chi_m T$ (Fig 5.9) values at temperatures higher than -35 K indicates ferromagnetic behavior of the complex. The effective magnetic moment μ_{eff} (s = 1/2 and g = 2.14) determined from the best fitted EPR data is 1.98; this μ_{eff} value agrees well with the μ_{eff} value for square planar geometry of Cu(II) ion.[36-37]

5.3.4. Computational Results

The optimization of the geometric structure of the complex was performed at B3LYP level of theory for evaluating the cluster models and computational methods. It is evident from the Fig 5.5 that the coordination environment of Cu(II) ion is in complete agreement with the structural geometry derived from single crystal X-ray diffraction.

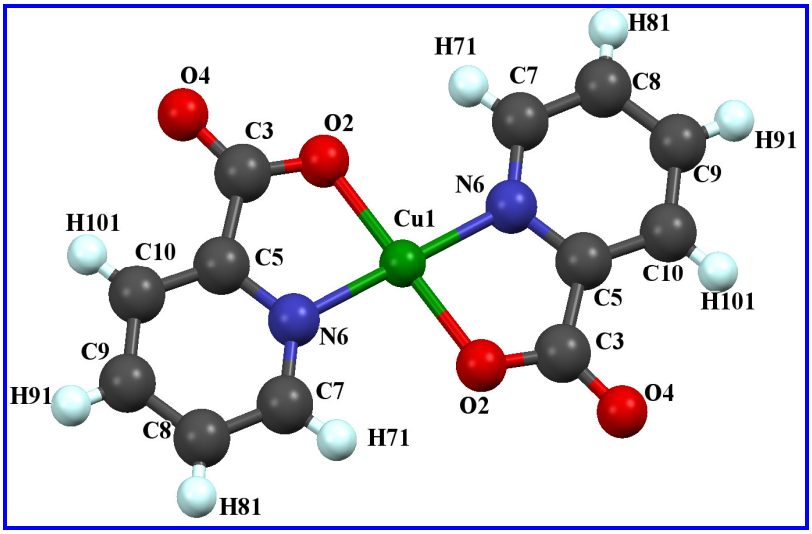

Fig 5.9. DFT optimized structure of the coordination sphere of the complex.

The Frontier Molecular Orbitals (HOMO and LUMO) can qualitatively predict the excitation properties and electron transport in the studied system, therefore, the parameter HOMO and LUMO can offer a reasonable prediction of molecular reactivity. Thus the energies of the HOMO and LUMO (shown in Fig 5.6) orbitals of the Cu(II) complex have been calculated using density functional theory(DFT) using Gaussian 09[38] programme. The energy of HOMO and LUMO orbitals has been found to be -6.5743 eV and -2.5021 eV respectively. Since the energy of HOMO and LUMO orbitals are negative and it indicates that the studied complex is stable.[39] Again the energy gap (ΔE) between HOMO and LUMO of the complex can be correlated with its stability and the energy gap (ΔE) = (E_{LUMO}-E_{HOMO}) for the studied system is found to be 4.0722 eV and

this large HOMO-LUMO gap reveals that the Cu(II) complex is highly stable.[40] This HOMO-LUMO energy gap falls in the visible region that corresponds to the blue colour of the crystal. However, the DFT based descriptors (HOMO-LUMO orbital energy) could be used in order to understand the structure and reactivity of molecule by calculating different properties such as Chemical potential (μ), Global hardness (η) and global electrophilicity power (ω). The HOMO-LUMO orbital energies are directly related to ionization energy (I= $-E_{HOMO}$) and electron affinity (A= $-E_{LUMO}$). Similarly, the chemical potential (μ), Global hardness (η) and global electrophilicity power (ω) are related to HOMO-LUMO orbital energies by the following relations: chemical potential (μ)= $(E_{HOMO}+E_{LUMO})/2$, Global hardness (η) = $(-E_{HOMO}+E_{LUMO})/2$ and global electrophilicity power (ω) = $\mu^2/2\eta$.

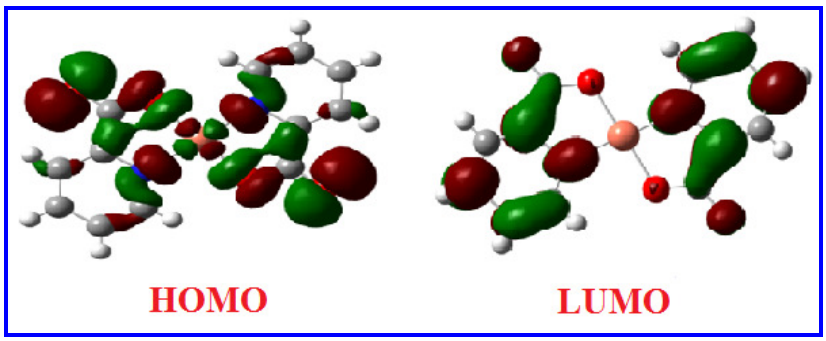

Fig 5.10. HOMO-LUMO of the title complex.

Alternatively, chemical potential (μ) and Global hardness (η) are given by the following relations: μ= -(I+A)/2 and η=(I-A)/2. Where I and A are the first ionization potential and electron affinity of the chemical species.[41] For the title compound, the values of first ionization potential (I), electron affinity (A), Chemical potential (μ), Global hardness (η) and electrophilicity power (ω) are -6.5743 eV, -2.5021 eV, -4.5382 eV, 2.036 eV and 5.06 eV respectively. Since the chemical potential (μ) of the studied complex is negative and it signifies that the compound is stable and do not decompose spontaneously into its elemental form. The HOMO-LUMO orbital energies, chemical potential (μ), Global hardness (η) and global electrophilicity power (ω) are summarized in Table 5.7.

Table 5.7. Physical parameters obtained theoretically for the complex.

Descriptors	Energy (eV)
E_{HOMO}	-6.5743
E_{LUMO}	-2.5021
ΔE	4.0722
Chemical potential(μ),	-4.5382
Global hardness (η)	2.036
Electrophilicity power (ω)	5.06

5.3.5. Hirschfeld surface analysis

In order to quantify the various intermolecular interactions, Hirschfeld surface analysis has been carried out for the synthesized complex and their associated two-dimensional fingerprint plots have been used to predict the possible intermolecular interactions. The descriptor d_{norm}, which incorporates two factors: (i) d_e, signifying the distance of any surface point nearest to the internal atoms, and (ii) d_i, signifying the distance of the surface point nearest to the exterior atoms and also with the van der Waals radii of the atoms has been used for mapping the Hirschfeld surface of a molecule.[42] The parameter d_{norm} is given by a mathematical expression as $d_{norm} = (d_i - r_i^{vdw}) / r_i^{vdw} + (d_e - r_e^{vdw}) / r_e^{vdw}$, where r_i^{vdw} and r_e^{vdw} are the van der walls raii of atoms. The parameter d_{norm} may have negative or positive value depending on the types of intermolecular contacts. If the value is positive, then the intermolecular contacts are shorter and if the value is positive the contacts are larger than the van der walls separations.[43] The descriptor d_{norm} displays a surface with bright red, white and blue spots for shortest contact, contact around the van der walls separation and devoid of close contacts respectively. Crystals with spherical atomic electron densities, the Hirschfeld surface is unique and it gives an idea about the intermolecular interactions occurring in the studied molecular crystals. In order for better visualization of the molecular moiety around which they are calculated, the surfaces have been shown as transparent. The molecular Hirschfeld surface for the Cu(II); d_{norm}, shape index and

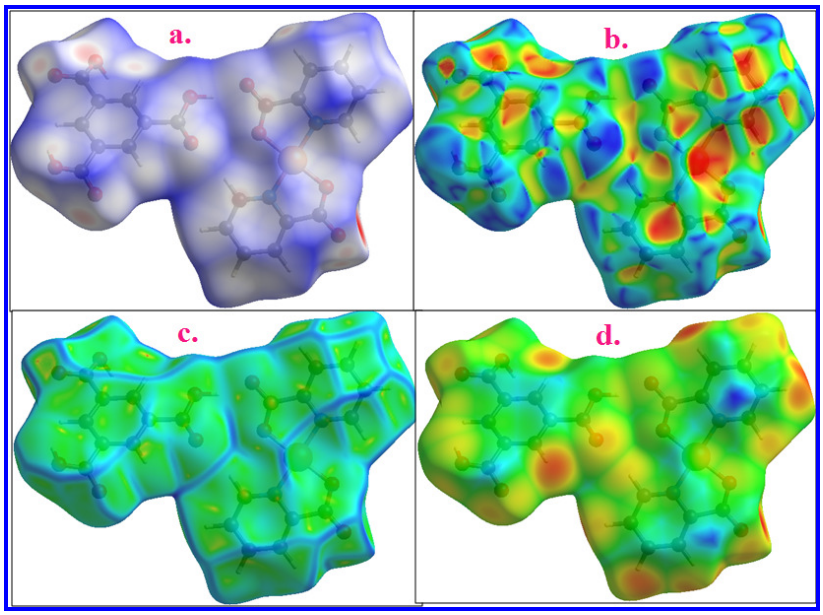

Fig 5.11. Molecular Hirschfeld surface: a) d_{norm} , b) shape index, c) curvedness and d) d_i for the complex.

curvedness for the Cu(II) complex is depicted in Fig. 5.11 respectively and mapped over d_{norm} ranges –0.7184 to 1.7801 Å, shape index ranges –1.0000 to 1.0000 Å, and curvedness ranges –4.0000 to 0.4000 Å, respectively. The d_{norm} mapping for the studied Cu(II) complex shows a bright red area in the Hirschfeld surfaces indicating the strong hydrogen bond interactions, such as O–H···O between coordinated/lattice water and carboxylate oxygen and these hydrogen bond interactions. The intermolecular interactions of the Cu(II) complex are shown in the 2D fingerprint plots shown in Fig 5.12. H…H contacts make the second largest contribution to the Hirshfeld surfaces (16.2%). The O…H/H..O makes the largest contributions to the Hirshfeld surfaces (19.1%) the CH regions while the green CH/HC interactions (9.6%).

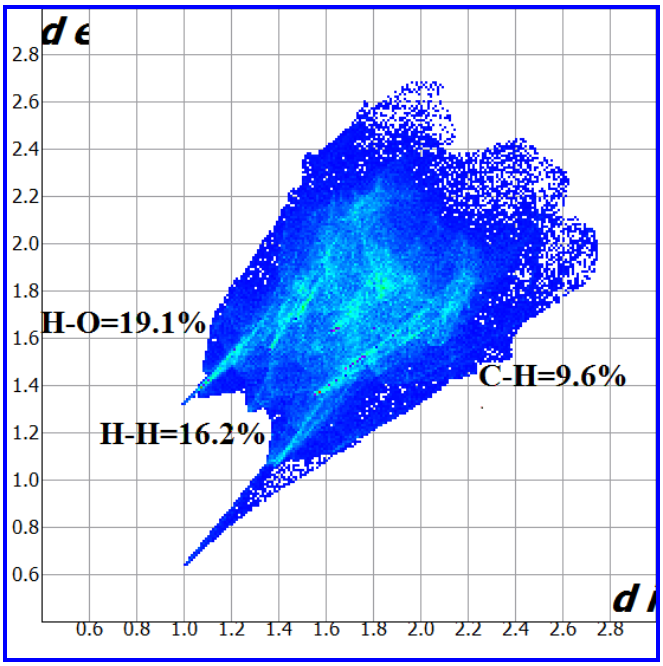

Fig 5.12. 2D fingerprint plots of the complex.

5.3.6. Thermogravimetric Analysis

The synthesized complex is air stable and insoluble in water. Thermal stability of the complex was studied using thermogravimetric technique in the temperature range 30-900 °C. The thermogram (shown in Fig 5.11) has mainly three weight loss stages.

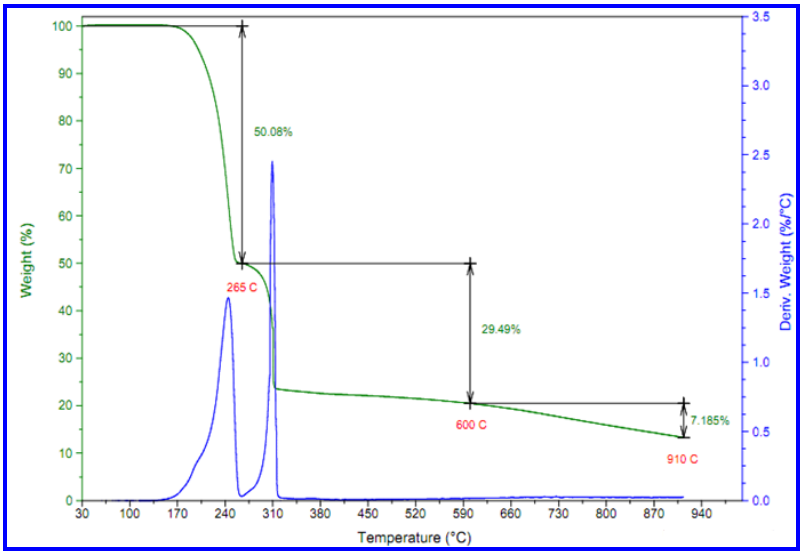

Fig 5.13. Thermogram of the complex in the temperature range 30-900 ^{o}C

The sample shows an initial mass loss of 50.08% (calcd: 56.9%) from 170 to 270 °C due to loss of non-coordinated TMA or its fragments. The DTG peak appears at 265 °C and the second weight loss stage occurs from 210 to 320 °C with a sharp weight loss of 29.49% (calcd: 33.54%) and consequently a DTG peak appears at around 310 °C. This sharp weight loss is probably due to loss of coordinated picolinate moieties. This stage is accompanied by subsequent weight loss of 7.185% due to the loss of organic fragments and finally the sample decomposes to corresponding metal oxide (CuO, calcd: 10.9%) at about 910 °C. So the complex has appreciable thermal stability at ambient to moderately high temperatures.

5.3.7. Scanning electron microscopic study

The FESEM analysis revealed that the crystals are like long rods with squared or rectangular cross sections with thickness of ~ 200µm. From Fig 5.12, it appears that the crystal has a rectangular or squared cross-section.

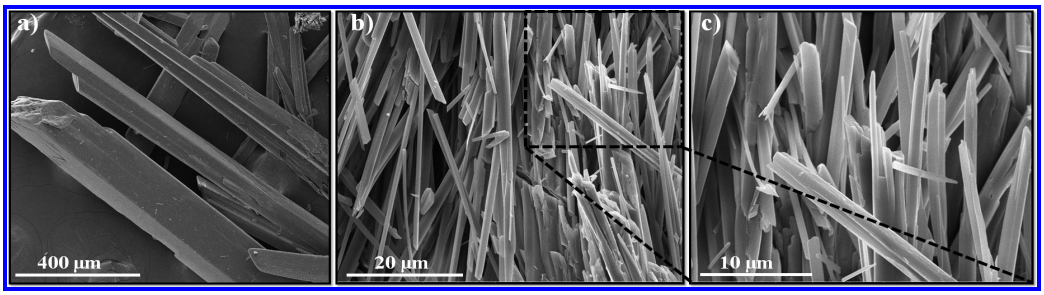

Fig 5.14. FESEM images of the complex: a) represents the large single crystals of thickness ~ 200 µm and several mm long, b) and c) show the individual grains of the crystal when ruptured along the length.

From the ruptured crystal it was found that the large single crystals are composed of long filamentous grains running along the length of the crystal with thickness ranging from 300 nm to 5µm.

5.4. Conclusion

The hydrothermally synthesized monoclinic Cu(II) hybrid complex is tetra coordinated with slightly distorted square planar geometry. The complex is stabilised by the extensive H-bonding involving TMA moiety. TGA and DFT studies justified its extreme stability. The crystalline nature and ferromagnetic behaviour was well supported by FESEM and SQUID respectively

References

[1]. M. Melnik, M. Kabesova, M. Koman, L. Macaskova and C. E. Holloway, *J. Coord. Chem.,* 2000, **50,** 177.

[2]. O. Kahn, *Molecular Magnetism*, VCH, New York, 1993.

[3]. F. E. Mabbs and D. Collison, *Electron Paramagnetic Resonance of d Transition Comounds*, Vol. 16, Elsevier, Amsterdam, 1992.

[4]. H. Deng, C.J. Doonan, H. Furukawa, R.B. Ferreira, J. Towne, C.B. Knobler, B. Wang and O.M. Yaghi, *Science*, 2010, **327**, 846.

[5]. M. Eddaoudi, H. Li and O.M. Yaghi, *J. Am. Chem.Soc.* 2000, **122**, 1391.

[6]. N. Emig, R. R´ eau H. Krautscheid, D. Fenske and G. Bertrand, *J. Am. Chem.Soc.* 1996, **118**, 5822.

[7]. A. Kamath, D. K. Mishra, D. Brahman, G. Pilet, B. Sinha and A. Tamang, *RSC Adv.*, 2016, **6**, 46030.

[8]. A. Shaver, J. B. Ng, D. A. Hall, B. S. Lum, and B. I. Posner, *Inorg. Chem*. 1993, **32,** 3109.

[9]. H. Sakurai, K. Fujii, H. Watanabe and H. Tamura, *Biochem. Biophys. Res.Commun*. 214 1995, **214**, 1095.

[10]. H. Sakurai, A. Tamura, T. Takino K. Ozutsumi, K. Kawabe, and Y. Koyima, *Inorg. React. Mech.,* 2000, **2**, 69.

[11]. K. H. Thompson and C. Orvig, *J. Chem. Soc., Dalton Trans.,* 2000, 2885.

[12]. E. Kiss, A. Bényei, and T. Kiss, *Polyhedron*, 2003, **22** 27.

[13]. M. Nakai, M. Obata, F. Sekiguchi, M. Kato, M. Shiro, A. Ichimura, I. Kinoshita, M. Mikuriya, T. Inohara, K. Kawabe, H. Sakurai, C. Orvig, and S. Yano, *J. Inorg. Biochem*. 2004, **98,** 105.

[14]. M. Nakai, F. Sekiguchi, M. Obata, C. Ohtsuki, Y. Adachi, H. Sakurai, C. Orvig, D. Rehder, and S. Yano, *J. Inorg. Biochem.,* 2005, **99**, 1275.

[15]. B. Zurowska, J. Mrozinski and Z. Ciunik, Polyhedron, 2007, **26**, 1251.

[16]. B. Zurowska, J. Ochocki, J. Mrozinski, Z. Ciunik and J. Reedijk, *Inorganica Chimica Acta*, 2004, **357**, 755.

[17]. H. Yasui, A. Tamura, T. Takino and H. Sakurai, *Journal of Inorganic Biochemistry*, 2002, **91**, 327.

[18]. M. Kalinowska, M. Borawska, R. Swislocka, J. Piekut and W. Lewandowski, *Journal of Molecular Structure*, 2007, **834-836**, 419.

[19]. S. Chaudhary, J. Pinkston, M.M. Rabile and J. D.Van Horn, *Journal of Inorganic Biochemistry*, 2005, **99**, 787.

[20]. B.M. Kukovec, I. Kodrin, V. Vojkovic and Z. Popovic, *Polyhedron*, 2013, **52**, 1349.

[21]. K.R. Ma, Y.L. Zhu, Q.F. Yin, H.Y. Hu and F. Ma, *J. Chem. Res.* 2010, **34**, 705.

[22]. M. Plater, A. Oberts, J. Marr, E.E. Lachowski and R.A. Howie, *J. Chem. Soc., Dalton Trans.,* 1998, 797.

[23]. M. Foo, S. Horkie, Y. Inubushi and S. Kitagwa, *Angew. Chem. Int. Ed.,* 2012, **51**, 6107.

[24]. JC Cramer, *Essentials of Computational Chemistry, Theories and Models, Second Edition, John Wiley & Sons Ltd, England,* 2004.

[25]. W Koch; MC Holthausen, *A chemist's guide to density functional theory. 2nd ed. New York:Wiley-VCH;* 2001.

[26]. A.J Cohen, P. Mori-Sánchez and W Yang, *Chem. Rev.,* 2012, **112**, 289.

[27]. A.D. Beck, *J.Chem. Phys.*, 1993, **98**, 568.

[28]. C. Lee, W. Yang, R. G. Parr, Phys. Rev B: Condens. *Matter Mater. Phys*. 1988, **37**, 785.

[29]. B. Mennucci, J. Tomasi, *J. Chem. Phys.,* 1997, **106(12)**, 5151.

[30]. K. Fukui, *Theory of Orientation and Stereoselection, Springer-Verlag, Berlin*, 1975, see also: K. Fukui, *Science*, 1987, **218**, 747.

[31]. K. Nakamoto, *Infrared and Raman Spectra of Inorganic and Coordination compounds*, *3rd ed*., Wiley, New York, 1997.

[32]. R. M. Silverstein and F. X. Webster, *Spectrometric Identification of Organic Compounds*, Wiley India Pvt Ltd., New Delhi, 6th edn, 2014.

[33]. D. M. Adams, Metal-*Ligand and Related Vibrations: A Critical Survey of the Infrared and Raman Spectra of Metallic and Organometallic Compounds*, Edward Arnold (Publisher) Ltd., London, 1967.

[34]. B Halliwell; JMC Gutteridge; *Free Radicals in Biology*, *Medicine*, 2nd edn., Clarendon Press, Oxford, 1989.

[35]. J. C. Bissey, R. Berger and Y. Servant, *Solid State Commun*, 1995, **93**, 243.

[36]. R. L. Dutta and A. Syamal, *Elements of Magnetochemistry*, Affiliated East-West Press Pvt Ltd, New Delhi, India, 2nd edn, 1993.

[37]. R. L. Dutta and A. Syamal, *Elements of Magnetochemistry*, Affiliated East-West Press Pvt Ltd, New Delhi, India, 2nd edn, 1993.

[38]. M. A. Spackman and D. Jayatilaka, *Cryst. Eng. Comm.* 2009, **11**, 19.

[39]. J. J. McKinnon, D. Jayatilaka and M.A. Spackman, *Chem Commun.,* 2007, 3814.

[40]. J. J. Koenderink and A. J. Van Doorn, *Image and Vision Computing*, 1992, **10**, 557.

[41]. J. J. McKinnon, M.A. Spackman and A.S. Mitchel, *Acta Crys. B,* 2004, **60,** 627

[42]. M.A. Spackman and D. Jayatilaka, *Cryst Eng. Comm,* 2009, **11**, 19.